RESEARCH ARTICLE

Stability of motor endplates is greater in the biceps than in the interossei in a rat model of obstetric brachial plexus palsy

Bo Li[1, 2], **Liang Chen**[1, 2, *], **Yu-Dong Gu**[1, 2]

1 Department of Hand Surgery, Huashan Hospital and Institutes of Biomedical Sciences, Fudan University, Shanghai, China
2 Shanghai Key Laboratory of Peripheral Nerve and Microsurgery, Shanghai, China

Funding: *This study was supported by the National Natural Science Foundation of China, No. 81672240 (to LC).*

Graphical Abstract

Changes of motor endplates, mRNA, and protein expression of acetylcholine receptor (AChR), rapsyn, and β-catenin in a rat model of obstetric brachial plexus palsy

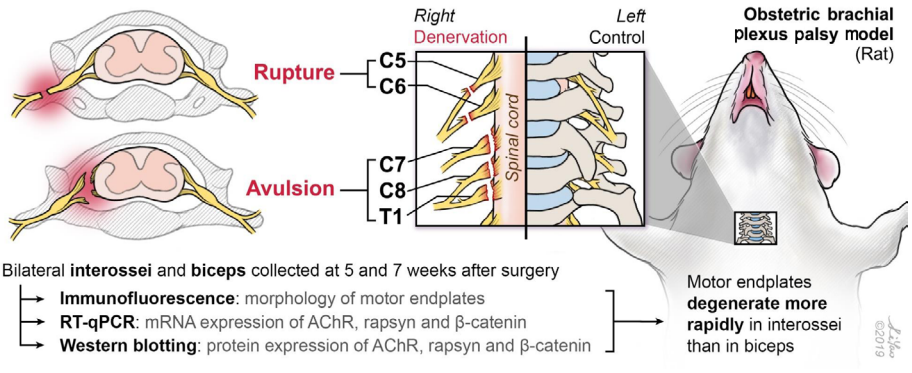

Correspondence to:
Liang Chen, MD, PhD, liangchen1960@163.com.

orcid:
0000-0002-4824-7454 (Liang Chen)

doi: *10.4103/1673-5374.276341*

Received: *August 12, 2019*
Peer review started: *August 22, 2019*
Accepted: *September 26, 2019*
Published online: *February 28, 2020*

Abstract

The time window for repair of the lower trunk is shorter than that of the upper trunk in patients with obstetric brachial plexus palsy. The denervated intrinsic muscles of the hand become irreversibly atrophic much faster than the denervated biceps. However, it is unclear whether the motor endplates of the denervated interosseous muscles degenerate more rapidly than those of the denervated biceps. In this study, we used a rat model of obstetric brachial plexus palsy of the right upper limb. C5–6 was lacerated distal to the intervertebral foramina, with concurrent avulsion of C7–8 and T1, with the left upper limb used as the control. Bilateral interossei and biceps were collected at 5 and 7 weeks. Immunofluorescence was used to assess the morphology of the motor endplates. Real-time quantitative polymerase chain reaction and western blot assay were used to assess mRNA and protein expression levels of acetylcholine receptor subunits (α, β and δ), rapsyn and β-catenin. Immunofluorescence microscopy showed that motor endplates in the denervated interossei were fragmented, while those in the denervated biceps were morphologically intact with little fragmentation. The number and area of motor endplates, relative to the control side, were significantly lower in the denervated interossei compared with the denervated biceps. mRNA and protein expression levels of acetylcholine receptor subunits (α, β and δ) were significantly lower, whereas β-catenin protein expression was higher, in the denervated interossei compared with the denervated biceps. The protein expression of rapsyn was higher in the denervated biceps than in the denervated interossei at 7 weeks. Our findings demonstrate that motor endplates of interossei are destabilized, whereas those of the biceps remain stable, in the rat model of obstetric brachial plexus palsy. All procedures were approved by the Experimental Animal Ethics Committee of Fudan University, China (approval No. DF-187) in January 2016.

Key Words: *acetylcholine receptor subunits; biceps; interossei; motor endplates; nerve regeneration; obstetric brachial plexus palsy; peripheral nerve injury*

Chinese Library Classification No. *R446; R363; R364*

Introduction

Obstetric brachial plexus palsy (OBPP) is a stretch injury of the brachial plexus during delivery (Pondaag et al., 2004; Barsaoui et al., 2017). Approximately 70% of patients with OBPP spontaneously recover by 4–6 months postnatally (Malessy and Pondaag, 2009; Shah et al., 2019); the remainder experience various sequelae of the upper limbs, necessitating reconstruction surgery. For nerve surgery, a longer operative delay is unfavorable for functional recovery (Mackinnon, 1989; Laurent et al., 1993). For OBPP, the clinical consensus is that the C8–T1 spinal nerves innervating the intrinsic muscles of the hand (IMH) should be reconstructed within a maximum of 3 months postnatally (Chuang et al., 2005). In contrast, for the C5–C6-innervated muscles of the upper arm, nerve grafting up to 30 months after birth might still provide functional improvement (Boom et al., 2000). In our previous study of a rat model of OBPP, in which the spinal nerves were reconstructed, we showed that atrophy of the intrinsic muscles of the forepaw (IMF) became irreversible far earlier than atrophy of the biceps, resulting in a shortened operative time window for nerve reconstruction of C8–T1 compared with C5–6 (Wu et al., 2013). Further studies using a rat model of OBPP without nerve reconstruction, in which the IMF are irreversibly atrophied and the biceps are reversibly atrophied, demonstrated that the denervated IMF and the denervated biceps show a unique expression profile of miRNAs (Pan et al., 2015) and mRNAs (Wu et al., 2016), respectively, and that the denervated IMF lacked self-repair potential compared with the denervated biceps (Wu et al., 2016). Furthermore, these findings suggest that the dysregulated miRNAs and mRNAs in these muscles might be associated with the structural and functional changes in the neuromuscular junctions (NMJs) after injury.

The NMJ is composed of the following five components: terminal Schwann cells, nerve endings that release neurotransmitters, a synaptic cleft, a postsynaptic membrane specialization containing the nicotinic acetylcholine receptor (AChR), and a sarcoplasm that provides structural and metabolic support for the postsynaptic region (Sanes and Lichtman, 2001; Wu et al., 2010; Mukund and Subramaniam, 2020). When the peripheral nerve is disconnected, its distal portion undergoes progressive (Wallerian) degeneration, characterized by a breakdown of axons and myelin, which peaks 4–6 weeks post-injury (Beirowski et al., 2004; Mu et al., 2018).

In rats with sciatic nerve transection, Adams et al. (1995) found that AChR mRNA expression in the gastrocnemius and tibialis anterior muscles peaked 7 days after denervation, and decreased to 10% of the control 6 months later. Ijkema-Paassen et al. (2002) showed that in rats with sciatic nerve transection, a few motor endplate fragments are detectable in the tibialis anterior muscle 4 weeks post-injury, but none by 7 weeks. After denervation, old AChRs are removed faster and replaced by new ones more slowly, while in innervated NMJs, the recycling of AChRs is in balance (Bruneau and Akaaboune, 2006). A recent study showed that early repair of sciatic nerve transection in mice and rats enhances functional reconstruction of NMJs in the target muscles, whereas delayed repair (beyond 1 month post-injury) only provides morphological reconstruction of NMJs without functional improvement (Sakuma et al., 2016).

Given that the IMH have a far shorter operative window than the biceps in OBPP, we hypothesized that degenerative changes occur more rapidly in the motor endplates in the IMH than in the biceps, resulting in the quicker irreversible atrophy of the denervated IMH compared with the biceps. In the present study, we tested this hypothesis using a rat model of OBPP in which the IMF are irreversibly atrophied, but atrophy of the biceps remains reversible (Pan et al., 2015; Wu et al., 2016).

Materials and Methods

Production of the rat model of OBPP and specimen collection

All procedures were approved by the Experimental Animal Ethics Committee of Fudan University, China (approval No. DF-187) in January 2016. Thirty-six 7-day-old male Sprague-Dawley rats weighing 11–13 g were provided by the Animal Science Department, Fudan University, China (license No. SYXK (Hu) 2014-0029).

Each rat was anesthetized intraperitoneally with 1% pentobarbital sodium (Sigma-Aldrich, St. Louis, MO, USA). While in the supine position, the right spinal nerves (C5–T1) were exposed via the supraclavicular route. A common type of OBPP was created. Briefly, C5–6 was lacerated distal to the intervertebral foramina, with concurrent avulsion of C7–T1, with no possibility of proximal nerve regeneration. To prevent nerve regeneration from C5–6, their proximal stumps were embedded into the surrounding tissue. The brachial plexus on the left remained uninjured to serve as control. All rats were caged under standard room temperature and humidity, with a 12-hour dark-light cycle and *ad libitum* access to food and fresh water.

The rats were sacrificed, and the bilateral interossei, one of the major IMF, and biceps were collected at 5 and 7 weeks after surgery (18 rats at each time point). This timeframe was selected according to our previous study of the OBPP rat model with nerve grafting, which showed that at 5 weeks after denervation, the IMF became irreversibly atrophic, whereas the biceps remained in a state of reversible atrophy (Wu et al., 2013). The criteria for successful modeling of OBPP were the following: (1) At 5 and 7 weeks after surgery, the right upper limb was thinner than the left upper limb; and (2) it had no function. Harvested specimens were stored at –80°C until analysis. Of the 18 rats analyzed at each time point, the interossei and biceps from 6 rats were used for immunofluorescence analysis of morphological changes in the motor endplates. Samples from another 6 rats were used to assess mRNA expression of AChRα, AChRβ and AChRδ subunits, as well as rapsyn and β-catenin, by real-time quantitative polymerase chain reaction (RT-qPCR). Samples from the remaining 6 rats were used to evaluate protein levels of these NMJ components by western blot assay.

Immunofluorescence labeling

Immunofluorescence labeling was performed to reveal the structure of NMJs at 5 and 7 weeks after surgery. AChR staining was used to assess the morphology of motor endplates, particularly as the postsynaptic muscle membrane is enriched in AChRs (Basu et al., 2015). Neurofilament staining was performed to show the motor nerve endings. The muscle tissue specimens were fixed overnight in 4% paraformaldehyde, dehydrated in 30% sucrose for 12 hours, and embedded in optimal cutting temperature compound. The tissue was sliced longitudinally using a microtome (Leica, Wetzlar, Germany), with 10 sections (20-μm thickness) harvested for morphological analysis of motor endplates. Sections were permeabilized with 0.3% Triton X-100 in phosphate-buffered saline for 30 minutes, and blocked with 3% bovine serum albumin in phosphate-buffered saline for 1 hour at room temperature. The sections were then incubated with rabbit anti-neurofilament heavy chain antibody (1:1000; Ab8135; Abcam, Cambridge, MA, USA) overnight at 4°C, followed by incubation with donkey polyclonal anti-rabbit IgG H&L (Alexa Fluor 647) (1:200; Ab150075; Abcam) (for neurofilament heavy chain) and α-Bungarotoxin-ATTO-488 (1:100; ALO-B-100-AG-0.1; Alomone, Jerusalem, Israel) (for AChRs) for 2 hours at 4°C. Finally, sections were mounted on slides with antifade reagents. Confocal fluorescence images were obtained on a Leica TCS SP8 microscope (Leica, Solms, Germany). Projections of maximal pixel intensity of Z-stacks were acquired with LAS-AF software (Leica).

The motor endplates for one section were counted, regardless of the orientation of motor endplates in relation to the focus plane of a microscope. For each muscle block, the number of motor endplates was evaluated semiquantitatively, and was expressed as the mean number of motor plates per section, which was calculated from five random sections from a total of 10. The percentage of endplates in the denervated muscle was calculated by dividing this value by that in the contralateral normal counterpart and multiplying by 100%. The area of motor endplates was measured using ImageJ software (NIH, Bethesda, MD, USA). The mean area of each of 50 endplates (10 chosen randomly from each of five sections) was calculated for the muscle tissue block. The percentage mean area of endplates in the denervated muscle was calculated by dividing the area by that in the contralateral normal muscle and multiplying by 100%.

RT-qPCR

AChR subunits (α, β and δ) are the main components of motor endplates, and rapsyn and β-catenin are key regulators of these subunits. cDNA templates were synthesized from 1 μg of RNA from each muscle sample at 5 and 7 weeks after surgery using SuperScript III Reverse Transcriptase (Invitrogen, Carlsbad, CA, USA). mRNA expression levels were determined by RT-qPCR using ABI SYBR Green PCR Master Mix (Applied Biosystems, Foster City, CA, USA) and a CFX96 thermocycler (Bio-Rad, Hercules, CA, USA). Primer pairs, synthesized by Sangon Biotech (Shanghai, China), are listed in **Table 1**. Relative mRNA expression levels were assessed for candidate genes from both denervated and contralateral normal muscles using the $2^{-\Delta\Delta CT}$ method and glyceraldehyde-3-phosphate dehydrogenase (GAPDH) as the internal control for normalization. The percentage expression of AChRα, AChRβ, AChRδ, rapsyn and β-catenin in the denervated muscle was calculated by dividing expression by the corresponding expression in the contralateral normal muscle and multiplying by 100%.

Table 1 Sequences of the primers used in the study

Gene	Sequence (5′–3′)	Product size (bp)
AChRα	Forward: CTC AAA TAC AGA AAG CAC TAG AAG	152
	Reverse: CAG GAA GCA GAC GAT AAT GAA CAG	
AChRβ	Forward: TGT TCA GCT TCA GCC TTC TTT	291
	Reverse: GGA GCC GGA CTT TCT TCA TAT	
AChRδ	Forward: GAG AAC GGT GAG TGG GAA ATA G	110
	Reverse: CGG ATG ATG AGG TAG AAG GTG A	
Rapsyn	Forward: GCT GAA GAG GTT GGA AAT AAG C	158
	Reverse: TCA CCA CAG AGG CCA CAG TAG A	
β-Catenin	Forward: ATG GAG CCG GAC AGA AAA GC	143
	Reverse: TGG GAG GTG TCA ACA TCT TCT T	
GAPDH	Forward: CCA TCA CTG CCA CTC AGA AGA	183
	Reverse: ATA CAT TGG GGG TAG GAA CAC	

AChR: Acetylcholine receptor; GAPDH: glyceraldehyde-3-phosphate dehydrogenase.

Western blot assay

Proteins were extracted from the bilateral interossei and biceps at 5 and 7 weeks after surgery at 4°C in radioimmunoprecipitation assay buffer containing protease and phosphatase inhibitors. Following centrifugation, the protein concentration in the supernatants was quantified using a bicinchoninic acid assay kit (Thermo Scientific, Waltham, MA, USA). For each sample, 30 μg of total protein was separated by 10% sodium dodecyl sulfate-polyacrylamide gel electrophoresis, and transferred to a polyvinylidene fluoride membrane. The membrane was blocked with 5% dried skim milk and incubated at 4°C for 12 hours with one of the following primary antibodies: rabbit anti-AChRα (1:1000; PAB12331; Abnova, Walnut, CA, USA), rabbit anti-AChRβ (1:1000; ab76159; Abcam), mouse anti-AChRδ (1:5000; NB120-2804; Novus Biologicals, Littleton, CO, USA), rabbit anti-rapsyn (1:1000; ab156002; Abcam), rabbit anti-β-catenin (1:5000; ab32572; Abcam) or rabbit anti-GAPDH (1:2500; ab9485; Abcam). After three washes with Tris-buffered saline-Tween for 15 minutes each, blots were incubated at room temperature for 2 hours with the corresponding horseradish perox-

idase-conjugated secondary antibody (goat anti-mouse or goat anti-rabbit; 1:5000; Millipore, Burlington, MA, USA). After three washes with Tris-buffered saline-Tween for 15 minutes each, immunoreactive bands were detected by chemiluminescence (Thermo Scientific) and quantified using ImageJ software, with GAPDH as an internal control. Finally, the percentage expression of AChRα, AChRβ, AChRδ, rapsyn and β-catenin in the denervated muscle was calculated by dividing the expression level by the corresponding expression level in the contralateral normal muscle and multiplying by 100%.

Statistical analysis

The median (p25–p75) was recorded for expression data. The Mann-Whitney *U*-test was used to measure differences between denervated interossei and denervated biceps using SPSS 19.0 software (SPSS, Armonk, NY, USA). $P < 0.05$ was considered statistically significant.

Results

Morphological and quantitative evaluation of motor endplates

Immunofluorescence staining for AChRs in muscle sections revealed that in normal interossei and biceps (**Figure 1A1–A3** and **C1–C3**), the motor endplate, a pretzel-like structure, was located in the center of the muscle fiber, and the motor nerve endings, with neurofilament labeling, were localized around the motor endplate. At 5 weeks after denervation, no motor nerve endings could be detected in interossei or biceps. In denervated interossei (**Figure 1B1–B3**), AChR clusters at the postsynaptic membrane were fragmented, and their contours were difficult to identify. However, in denervated biceps (**Figure 1D1–D3**), AChR clusters were morphologically intact with little fragmentation, although they were shrunken. In interossei and biceps that had been denervated for 7 weeks, fragmentation of the interossei motor endplates worsened (**Figure 2B1–B3**), while in comparison, the biceps motor endplates remained mostly intact (**Figure 2D1–D3**).

Compared with the normal side, the number and area of the motor endplates were markedly reduced in the denervated interossei and biceps. The percentage mean number of endplates per section relative to the contralateral normal counterpart, was significantly lower in the denervated interossei than in the denervated biceps, 5 weeks ($P < 0.01$) and 7 weeks ($P < 0.01$) after denervation (**Table 2**). Furthermore, the percentage mean area per endplate relative to the contralateral normal counterpart was significantly lower in the denervated interossei than in the denervated biceps, 5 weeks ($P < 0.01$) and 7 weeks ($P < 0.01$) after denervation (**Table 2**).

mRNA expression levels of AChRα, AChRβ, AChRδ, rapsyn and β-catenin

The expression levels of AChRα, AChRβ and AChRδ mRNA (relative to the corresponding normal control) were significantly lower in denervated interossei than in denervated biceps, 5 weeks ($P < 0.01$) and 7 weeks ($P < 0.01$) after denervation. The expression of rapsyn mRNA was not significantly different between the two denervated muscles at 5 weeks ($P > 0.05$) or 7 weeks ($P > 0.05$). The expression of β-catenin mRNA was significantly higher in denervated interossei compared with denervated biceps at 5 weeks ($P < 0.01$), but not at 7 weeks ($P > 0.05$) (**Figure 3**).

Protein expression levels of AChRα, AChRβ, AChRδ, rapsyn and β-catenin

The expression levels of AChRα, AChRβ and AChRδ, relative to the contralateral normal muscles, were significantly lower in the denervated interossei than in the denervated biceps at 5 weeks ($P < 0.01$ or $P < 0.05$) and 7 weeks ($P < 0.01$) after denervation. The expression of rapsyn protein, relative to the corresponding normal control, was significantly lower in the denervated interossei than in the denervated biceps at 5 weeks ($P < 0.01$), but not at 7 weeks ($P > 0.05$). The expression of β-catenin protein, relative to the normal control, was significantly higher in the denervated interossei than in the denervated biceps at 5 weeks ($P < 0.01$) and 7 weeks ($P < 0.01$) (**Figure 4**).

Table 2 Comparison of percentage of number and area of motor endplates between denervated interossei and denervated biceps in rats

		Interossei			Biceps		
		Denervated side	Normal side	Percentage	Denervated side	Normal side	Percentage
Number of MEP	5 weeks	31.7 (27.7–33.0)	72.9 (62.5–74.5)	44.1* (41.7–45.9)	34.0 (30.1–36.5)	57.3 (54.5–59.9)	58.0* (56.2–61.3)
	7 weeks	20.3 (19.9–21.8)	72.1 (68.5–74.8)	29.1* (27.3–31.4)	22.9 (21.7–24.4)	58.5 (56.4–63.2)	38.8* (36.7–40.4)
Area of MEP	5 weeks	25.7 (22.6–27.9)	84.9 (77.5–93.8)	29.7* (11.8–17.4)	60.2 (56.9–65.9)	145 (138.9–156.9)	41.8* (38.8-43.5)
	7 weeks	13.4 (11.5–14.1)	88.3 (82.5–94.6)	14.4* (13.2–16.4)	40.3 (36.4–43.9)	156.6 (147.5–174.1)	27.1* (22.2–27.8)

Percentage: Divide the value on the denervated side by that of the normal side, and multiply by 100%. All data are expressed as median with interquartile range. Number of MEP: The average number of motor endplates per section that obtained from the average of the 5 sections chosen to be every 2 of the 10 sections. Area of MEP: The average area of one motor endplate that gained from the average of 50 motor endplates chosen equally and randomly from those five sections. *$P < 0.01$ (Percentage of number (or area) of MEP in interossei/biceps). MEP: Motor endplates.

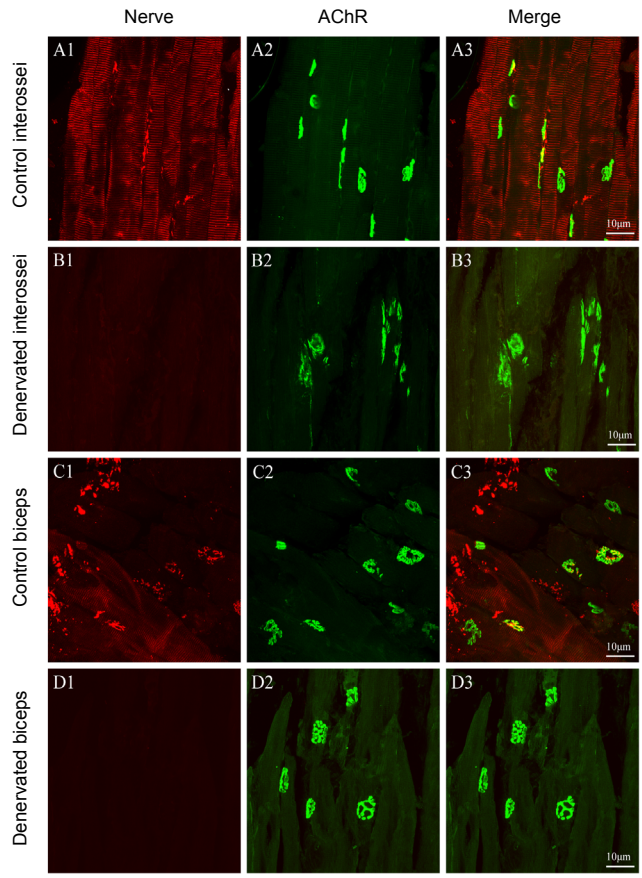

Figure 1 Confocal images of motor endplates of interossei and biceps 5 weeks after denervation.

In normal interossei (A1–A3) and biceps (C1–C3), motor nerve fibers are observed near motor endplates, which show a classical pretzel-like structure. In the denervated interossei (B1–B3), motor endplates are fragmented and their contours are obscured. However, in the denervated biceps (D1–D3), motor endplates are intact with little fragmentation, although they appear shrunken. Red: Neurofilament; green: α-bungarotoxin. Scale bars: 10 μm.

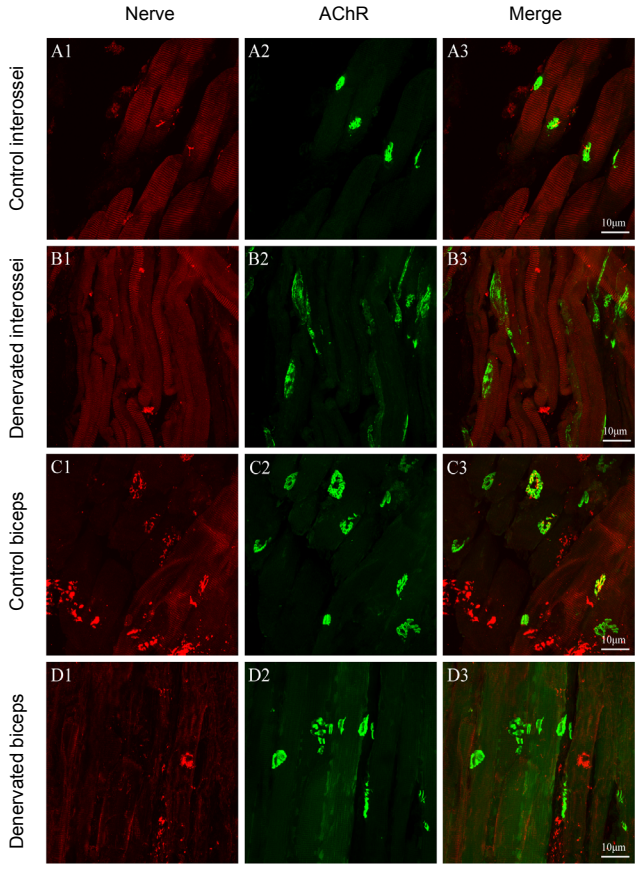

Figure 2 Confocal images of motor endplates of interossei and biceps 7 weeks after denervation.

In normal interossei (A1–A3) and biceps (C1–C3), motor nerve fibers are observed near motor endplates, which show a classical pretzel-like structure. In denervated interossei (B1–B3), fragmentation of motor endplates worsened. In the denervated biceps (D1–D3), the morphology of motor endplates is still mainly intact. Red: neurofilament; green: α-bungarotoxin. Scale bars: 10 μm.

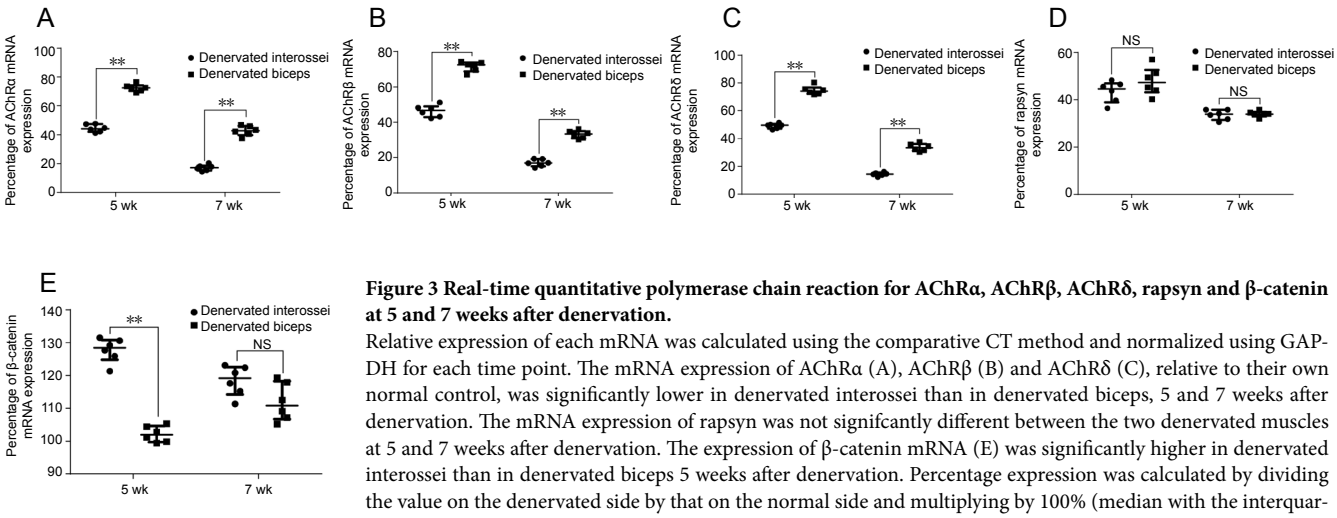

Figure 3 Real-time quantitative polymerase chain reaction for AChRα, AChRβ, AChRδ, rapsyn and β-catenin at 5 and 7 weeks after denervation.

Relative expression of each mRNA was calculated using the comparative CT method and normalized using GAPDH for each time point. The mRNA expression of AChRα (A), AChRβ (B) and AChRδ (C), relative to their own normal control, was significantly lower in denervated interossei than in denervated biceps, 5 and 7 weeks after denervation. The mRNA expression of rapsyn was not signifcantly different between the two denervated muscles at 5 and 7 weeks after denervation. The expression of β-catenin mRNA (E) was significantly higher in denervated interossei than in denervated biceps 5 weeks after denervation. Percentage expression was calculated by dividing the value on the denervated side by that on the normal side and multiplying by 100% (median with the interquartile range, $n = 6$; Mann–Whitney U-test); $^{**}P < 0.01$. AChR: Acetylcholine receptor; NS: not significant.

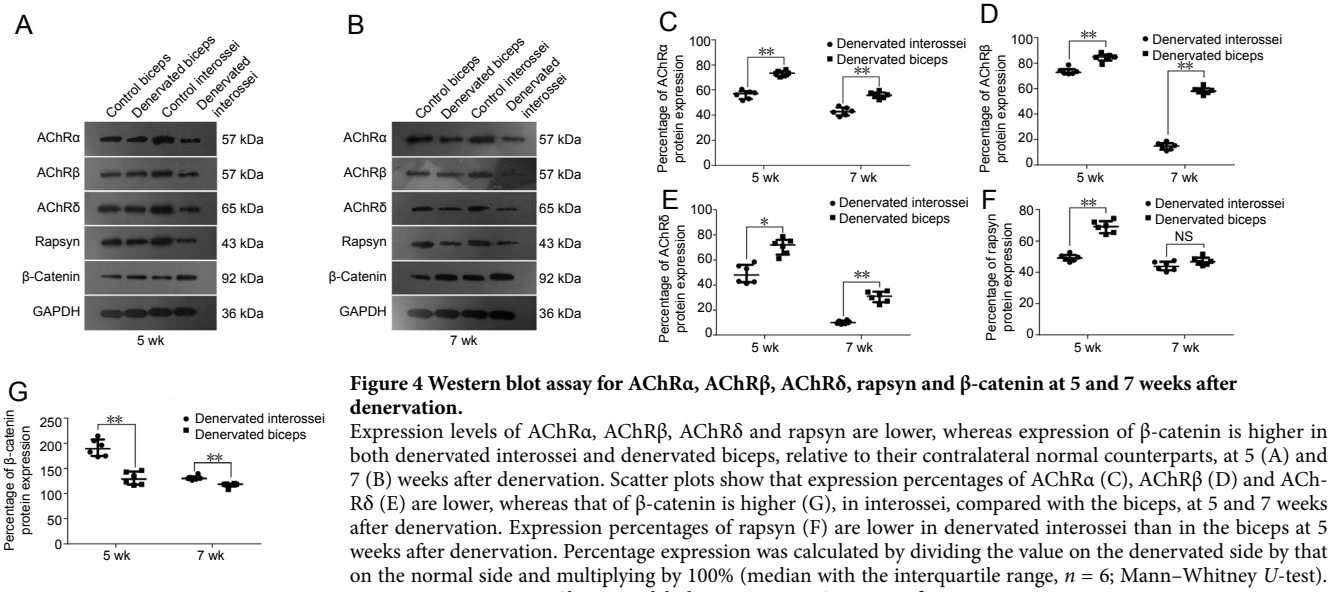

Figure 4 Western blot assay for AChRα, AChRβ, AChRδ, rapsyn and β-catenin at 5 and 7 weeks after denervation.

Expression levels of AChRα, AChRβ, AChRδ and rapsyn are lower, whereas expression of β-catenin is higher in both denervated interossei and denervated biceps, relative to their contralateral normal counterparts, at 5 (A) and 7 (B) weeks after denervation. Scatter plots show that expression percentages of AChRα (C), AChRβ (D) and AChRδ (E) are lower, whereas that of β-catenin is higher (G), in interossei, compared with the biceps, at 5 and 7 weeks after denervation. Expression percentages of rapsyn (F) are lower in denervated interossei than in the biceps at 5 weeks after denervation. Percentage expression was calculated by dividing the value on the denervated side by that on the normal side and multiplying by 100% (median with the interquartile range, $n = 6$; Mann–Whitney U-test). $*P < 0.05$, $**P < 0.01$. AChR: Acetylcholine receptor; NS: not significant.

Discussion

At the early stage after denervation, motor endplates remain intact anatomically because of their intrinsic ability to prepare for re-innervation. For example, in mice with transection of the sciatic nerve, motor endplates in the target muscles can remain morphologically intact 1 month after denervation, although degenerative changes appear at 2 months (Kurimoto et al., 2015). In the present study, the motor endplates were imaged by immunofluorescence with α-bungarotoxin, which binds AChRs. It was previously reported that AChRs may diffuse throughout the entire muscle fiber after denervation (Miledi and Slater, 1968; Stanley and Drachman, 1981), and that the extra-junctional AChRs are diffusely distributed and no longer localized to motor endplates (Hartzell and Fambrough, 1972), whereas regenerating axons always reoccupy the original synaptic sites (Purves and Lichtman, 1987; Kang and Lichtman, 2013). Here, we found that the motor endplates of the denervated biceps displayed an intact morphology, while those in the denervated interossei appeared fragmented. This suggests that AChRs in the biceps remain localized to their original synaptic sites. Furthermore, the number and area of the motor endplates, relative to the uninjured side, were much lower in the denervated interossei than in the denervated biceps. Thus, together with our previous study, the current findings suggest that the motor endplates of the denervated IMH exhibit a lower ability for self-repair compared with the denervated biceps, resulting in a relatively reduced potential for re-innervation.

The AChR in motor endplates of skeletal muscles is a pentamer composed of 2α, β, γ and δ subunits (Witzemann et al., 1989; Adams et al., 1995; Foucault-Fruchard et al., 2018; Weng et al., 2018; Das et al., 2019). In innervated muscles, the expression of the AChR subunits may be reduced by neuronal factors and muscular activity induced by nerve firing, in a negative feedback effect (Witzemann et al., 1991). In rats with nerve transection, denervation results in upregulation of most AChR subunits in the target muscle, peaking at 7 days post-injury, possibly by interrupting the negative feedback. However, the AChR subunits are downregulated below baseline from one month onwards, likely because the progressive atrophy of the denervated muscles may reduce the availability of AChR subunits (Ma et al., 2005, 2007; Shen et al., 2006). In the present study, using rats at 7 days of age, we only examined the expression of AChRα, β and δ subunits, because they are expressed more stable than the γ and δ subunits shortly after birth (Witzemann et al., 1989). The α, β and δ subunits were downregulated in both the interossei and biceps at 5 and 7 weeks after denervation, consistent with previous studies (Adams et al., 1995; Ma et al., 2007). The relative mRNA and protein expression levels of the α, β and δ subunits were reduced, while β-catenin protein expression was increased in the denervated interossei, compared with the denervated biceps, at 5 and 7 weeks. Rapsyn, a synaptic protein, is necessary for the clustering of AChRs and the formation of NMJs (Apel et al., 1997; Phillips et al., 1997; Huebsch and Maimone, 2003; Chen et al., 2016). β-Catenin is a key signaling molecule in the Wnt pathway. Activation of β-catenin induces its aggregation in the cell membrane and cytoplasm, as well as its translocation to the nucleus to activate various target genes (Cisternas et al., 2014). A study of mice with sciatic nerve laceration showed that β-catenin mRNA was upregulated around AChRs in denervated target muscles (Kurimoto et al., 2015) and inhibited AChR clustering by suppressing rapsyn expression (Wang et al., 2008). Our current findings suggest that in denervated interossei, the AChR is downregulated because of a lack of subunit availability, compared with the denervated biceps. Furthermore, the subunits are less likely to combine to form active receptors in denervated interossei, compared with denervated biceps. These changes likely contribute to the destabilization of endplates in the denervated interossei.

In our previous study using the OBPP rat model, in which the proximal stump of the C6 spinal nerve was grafted to the

ulnar nerve and that of C5 to the musculocutaneous nerve, we found that the IMF remained uninnervated at 5 weeks, while the biceps were reinnervated even at 10 weeks (Wu et al., 2013). Accordingly, regenerated motor endplates were much fewer in the IMF than in the biceps.

In a study using a mouse model of motor neuron disease, NMJs of IIb (fast-twitch) fibers were found to be lost more easily than NMJs of the IIa (fast-twitch) and I (slow-twitch) fibers, and botulinum toxin A-induced plasticity was much poorer in IIb fibers compared with the other fibers (Frey et al., 2000). Lumbrical muscles, one of the major muscles of the IMF, whose function is very similar to that of the interossei, are almost all composed of type II fibers (Russell et al., 2015), of which IIb fibers account for 80% of the total (Ridge and Rowlerson, 1996). In contrast, in the biceps, the type I and IIa fibers account for up to 55% of total muscle fibers (Fuentes et al., 1998). Thus, the much greater ratio of IIb fibers in the interossei might be the major factor contributing to the comparatively rapid degeneration of motor endplates in the interossei after denervation. Functionally, the IMH are still immature a year postnatally, whereas the biceps is mature at birth (Zafeiriou, 2004). Immature synapses during development are more vulnerable to damage caused by the blocking of nerve-evoked activities, compared with mature synapses (Pun et al., 2002). We conjecture that the relatively immature status of the IMH may also contribute to the comparatively rapid motor endplate degeneration and the irreversible atrophy in these muscles in OBPP.

In summary, the motor endplates of denervated interossei were rapidly destabilized, while those of the denervated biceps remained comparatively stable, in a rat model of OBPP. AChR mRNA and protein expression levels were significantly lower, whereas β-catenin protein expression was higher, in the denervated interossei compared with the denervated biceps. These findings suggest that in OBPP, the self-repair potential of motor endplates is lower in the denervated IMH than in the denervated biceps.

Acknowledgments: *We thank Li Yao from Howard Hughes Medical Institute (Bethesda, MD, USA) for her assistance with the OBPP model illustrations.*

Author contributions: *Study design: LC; experimental implementation: BL; data analysis and paper writing: BL and LC; analysis with constructive discussions: YDG. All authors approved the final version of the paper.*

Conflicts of interest: *The authors declare that there are no conflicts of interest associated with this manuscript.*

Financial support: *This study was supported by the National Natural Science Foundation of China, No. 81672240 (to LC). The funding source had no role in study conception and design, data analysis or interpretation, paper writing or deciding to submit this paper for publication.*

Institutional review board statement: *All procedures were approved by the Experimental Animal Ethics Committee of Fudan University, China (approval No. DF-187) in January 2016. The experimental procedure followed the United States National Institutes of Health Guide for the Care and Use of Laboratory Animals (NIH Publication No. 85-23, revised 1996).*

Copyright license agreement: *The Copyright License Agreement has been signed by all authors before publication.*

Data sharing statement: *Datasets analyzed during the current study are available from the corresponding author on reasonable request.*

Plagiarism check: *Checked twice by iThenticate.*

Peer review: *Externally peer reviewed.*

Open peer reviewer: *Annas Al-Sharea, Baker IDI Heart and Diabetes Institute, Australia.*

Additional file: *Open peer review report 1.*

References

Adams L, Carlson BM, Henderson L, Goldman D (1995) Adaptation of nicotinic acetylcholine receptor, myogenin, and MRF4 gene expression to long-term muscle denervation. J Cell Biol 131:1341-1349.

Apel ED, Glass DJ, Moscoso LM, Yancopoulos GD, Sanes JR (1997) Rapsyn is required for MuSK signaling and recruits synaptic components to a MuSK-containing scaffold. Neuron 18:623-635.

Barsaoui M, Safi H, Said W, Nessib MN (2017) Nerve surgery in obstetric brachial plexus palsy, report of 68 cases. Tunis Med 95:196-200.

Basu S, Sladecek S, Martinez de la Peña y Valenzuela I, Akaaboune M, Smal I, Martin K, Galjart N, Brenner HR (2015) CLASP2-dependent microtubule capture at the neuromuscular junction membrane requires LL5β and actin for focal delivery of acetylcholine receptor vesicles. Mol Biol Cell 26:938-951.

Beirowski B, Berek L, Adalbert R, Wagner D, Grumme DS, Addicks K, Ribchester RR, Coleman MP (2004) Quantitative and qualitative analysis of Wallerian degeneration using restricted axonal labelling in YFP-H mice. J Neurosci Methods 134:23-35.

Bonetti LV, Malysz T, Ilha J, Barbosa S, Achaval M, Faccioni-Heuser MC (2017) The effects of two different exercise programs on the ultrastructural features of the sciatic nerve and soleus muscle after sciatic crush. Anat Rec (Hoboken) 300:1654-1661.

Boome (2000) Traumatic branchial plexus injury. In: The growing hand: diagnosis and management of the upper extremity in children (Gupta A, Kay SPJ, Scheker LR, eds), pp 653-655. London, UK: Mosby.

Bruneau EG, Akaaboune M (2006) The dynamics of recycled acetylcholine receptors at the neuromuscular junction in vivo. Development 133:4485-4493.

Budnik V, Salinas PC (2011) Wnt signaling during synaptic development and plasticity. Curr Opin Neurobiol 21:151-159.

Chen PJ, Martinez-Pena YVI, Aittaleb M, Akaaboune M (2016) AChRs are essential for the targeting of rapsyn to the postsynaptic membrane of NMJs in living mice. J Neurosci 36:5680-5685.

Chuang DC, Mardini S, Ma HS (2005) Surgical strategy for infant obstetrical brachial plexus palsy: experiences at chang gung memorial hospital. Plast Reconstr Surg 116:132-144.

Cisternas P, Henriquez JP, Brandan E, Inestrosa NC (2014) Wnt signaling in skeletal muscle dynamics: myogenesis, neuromuscular synapse and fibrosis. Mol Neurobiol 49:574-589.

Das BC, Dasgupta S, Ray SK (2019) Potential therapeutic roles of retinoids for prevention of neuroinflammation and neurodegeneration in Alzheimer's disease. Neural Regen Res 14:1880-1892.

Feng X, Zhang T, Ralston E, Ludlow CL (2012) Differences in neuromuscular junctions of laryngeal and limb muscles in rats. Laryngoscope 122:1093-1098.

Foad SL, Mehlman CT, Foad MB, Lippert WC (2009) Prognosis following neonatal brachial plexus palsy: an evidence-based review. J Child Orthop 3:459-463.

Foucault-Fruchard L, Tronel C, Bodard S, Gulhan Z, Busson J, Chalon S, Antier D (2018) Alpha-7 nicotinic acetylcholine receptor agonist treatment in a rat model of Huntington's disease and involvement of heme oxygenase-1. Neural Regen Res 13:737-741.

Frey D, Schneider C, Xu L, Borg J, Spooren W, Caroni P (2000) Early and selective loss of neuromuscular synapse subtypes with low sprouting competence in motoneuron diseases. J Neurosci 20:2534-2542.

Fuentes I, Cobos AR, Segade LA (1998) Muscle fibre types and their distribution in the biceps and triceps brachii of the rat and rabbit. J Anat 192:203-210.

Gordon MD, Nusse R (2006) Wnt signaling: multiple pathways, multiple receptors, and multiple transcription factors. J Biol Chem 281:22429-22433.

Hartzell HC, Fambrough DM (1972) Acetylcholine receptors. Distribution and extrajunctional density in rat diaphragm after denervation correlated with acetylcholine sensitivity. J Gen Physiol 60:248-262.

Hoeksma AF, ter SAM, Nelissen RG, van Ouwerkerk WJ, Lankhorst GJ, de Jong BA (2004) Neurological recovery in obstetric brachial plexus injuries: an historical cohort study. Dev Med Child Neurol 46:76-83.

Huebsch KA, Maimone MM (2003) Rapsyn-mediated clustering of acetylcholine receptor subunits requires the major cytoplasmic loop of the receptor subunits. J Neurobiol 54:486-501.

Ijkema-Paassen J, Meek MF, Gramsbergen A (2002) Reinnervation of muscles after transection of the sciatic nerve in adult rats. Muscle Nerve 25:891-897.

Kang H, Lichtman JW (2013) Motor axon regeneration and muscle reinnervation in young adult and aged animals. J Neurosci 33:19480-19491.

Kurimoto S, Jung J, Tapadia M, Lengfeld J, Agalliu D, Waterman M, Mozaffar T, Gupta R (2015) Activation of the Wnt/β-catenin signaling cascade after traumatic nerve injury. Neuroscience 294:101-108.

Laurent JP, Lee R, Shenaq S, Parke JT, Solis IS, Kowalik L (1993) Neurosurgical correction of upper brachial plexus birth injuries. J Neurosurg 79:197-203.

Ma J, Shen J, Garrett JP, Lee CA, Li Z, Elsaidi GA, Ritting A, Hick J, Tan KH, Smith TL, Smith BP, Koman LA (2007) Gene expression of myogenic regulatory factors, nicotinic acetylcholine receptor subunits, and GAP-43 in skeletal muscle following denervation in a rat model. J Orthop Res 25:1498-1505.

Ma J, Shen J, Garrett JP, Lee CA, Li Z, Elsaidi GA, Ritting A, Hick J, Tan KH, Smith TL, Smith BP, Koman LA (2005) Gene expression of nAChR, SNAP-25 and GAP-43 in skeletal muscles following botulinum toxin A injection: a study in rats. J Orthop Res 23:302-309.

Mackinnon SE (1989) New directions in peripheral nerve surgery. Ann Plast Surg 22:257-273.

Malessy MJ, Pondaag W (2009) Obstetric brachial plexus injuries. Neurosurg Clin N Am 20:1-14.

Miledi R, Slater CR (1968) Electrophysiology and electron-microscopy of rat neuromuscular junctions after nerve degeneration. Proc R Soc Lond B Biol Sci 169:289-306.

Mu L, Chen J, Li J, Nyirenda T, Fowkes M, Sobotka S (2018) Immunohistochemical detection of motor endplates in the long-term denervated muscle. J Reconstr Microsurg 34:348-358.

Mukund K, Subramaniam S (2020) Skeletal muscle: A review of molecular structure and function, in health and disease. Wiley Interdiscip Rev Syst Biol Med 12:e1462.

Pan F, Chen L, Ding F, Zhang J, Gu YD (2015) Expression profiles of MiRNAs for intrinsic musculature of the forepaw and biceps in the rat model simulating irreversible muscular atrophy of obstetric brachial plexus palsy. Gene 565:268-274.

Phillips WD, Vladeta D, Han H, Noakes PG (1997) Rapsyn and agrin slow the metabolic degradation of the acetylcholine receptor. Mol Cell Neurosci 10:16-26.

Pondaag W, Malessy MJ, van Dijk JG, Thomeer RT (2004) Natural history of obstetric brachial plexus palsy: a systematic review. Dev Med Child Neurol 46:138-144.

Pun S, Sigrist M, Santos AF, Ruegg MA, Sanes JR, Jessell TM, Arber S, Caroni P (2002) An intrinsic distinction in neuromuscular junction assembly and maintenance in different skeletal muscles. Neuron 34:357-370.

Purves D, Lichtman JW (1987) Synaptic sites on reinnervated nerve cells visualized at two different times in living mice. J Neurosci 7:1492-1497.

Ridge RM, Rowlerson A (1996) Motor units of juvenile rat lumbrical muscles and fibre type compositions of the glycogen-depleted component. J Physiol 497:199-210.

Russell KA, Ng R, Faulkner JA, Claflin DR, Mendias CL (2015) Mouse forepaw lumbrical muscles are resistant to age-related declines in force production. Exp Gerontol 65:42-45.

Sakuma M, Gorski G, Sheu SH, Lee S, Barrett LB, Singh B, Omura T, Latremoliere A, Woolf CJ (2016) Lack of motor recovery after prolonged denervation of the neuromuscular junction is not due to regenerative failure. Eur J Neurosci 43:451-462.

Sanes JR, Lichtman JW (2001) Induction, assembly, maturation and maintenance of a postsynaptic apparatus. Nat Rev Neurosci 2:791-805.

Shah AS, Kalish LA, Bae DS, Peljovich AE, Cornwall R, Bauer AS, Waters PM; Treatment and Outcomes of Brachial Plexus Injuries (TOBI) Study Group (2019) Early predictors of microsurgical reconstruction in brachial plexus birth palsy. Iowa Orthop J 39:37-43.

Shen J, Ma J, Lee C, Smith BP, Smith TL, Tan KH, Koman LA (2006) How muscles recover from paresis and atrophy after intramuscular injection of botulinum toxin A: study in juvenile rats. J Orthop Res 24:1128-1135.

Wang J, Ruan NJ, Qian L, Lei WL, Chen F, Luo ZG (2008) Wnt/beta-catenin signaling suppresses Rapsyn expression and inhibits acetylcholine receptor clustering at the neuromuscular junction. J Biol Chem 283:21668-21675.

Weng J, Wang YH, Li M, Zhang DY, Jiang BG (2018) GSK3β inhibitor promotes myelination and mitigates muscle atrophy after peripheral nerve injury. Neural Regen Res 13:324-330.

Witzemann V, Barg B, Criado M, Stein E, Sakmann B (1989) Developmental regulation of five subunit specific mRNAs encoding acetylcholine receptor subtypes in rat muscle. FEBS Lett 242:419-424.

Witzemann V, Brenner HR, Sakmann B (1991) Neural factors regulate AChR subunit mRNAs at rat neuromuscular synapses. J Cell Biol 114:125-141.

Wu H, Xiong WC, Mei L (2010) To build a synapse: signaling pathways in neuromuscular junction assembly. Development 137:1017-1033.

Wu JX, Chen L, Ding F, Chen LZ, Gu YD (2016) mRNA expression characteristics are different in irreversibly atrophic intrinsic muscles of the forepaw compared with reversibly atrophic biceps in a rat model of obstetric brachial plexus palsy (OBPP). J Muscle Res Cell Motil 37:17-25.

Wu JX, Chen L, Ding F, Gu YD (2013) A rat model study of atrophy of denervated musculature of the hand being faster than that of denervated muscles of the arm. J Muscle Res Cell Motil 34:15-22.

Zafeiriou DI (2004) Primitive reflexes and postural reactions in the neurodevelopmental examination. Pediatr Neurol 31:1-8.

P-Reviewer: Al-Sharea A; C-Editor: Zhao M; S-Editors: Wang J, Li CH; L-Editors: Patel B, Hindle A, Qiu Y, Song LP; T-Editor: Jia Y